

## Supporting Information

### Synchronously Chemically Closed-loop and High-Performance Approach for Furan-based Copolyester with Robustness, High Gas Barrier, High Puncture Resistance

Xing-Liang Li, Teng Fu\*, Zheng-Ming Li, Yao Li, Xiu-Li Wang, and Yu-Zhong Wang\*

**Abstract:** Utilizing bio-based resources is an essential part of the sustainable development of plastics. Meanwhile, the end-of-life options of this bio-based plastic must be considered to avoid contributing to the accumulation of plastic waste. To address the problem of end-of-life plastics and trade-off between chemical closed-loop recycling and high-performance, targeted selection of monomers and a method for the preparation of high-performance linear polyesters that can be rapidly closed-loop recycling without the addition of additional organic solvents under mild conditions are necessary. Herein, we report strategies for synchronously constructing chemical closed-loop and achieving high performance, by linear furan-based poly(butylene furandicarboxylate-diethylene glycol) (PBD<sub>y</sub>F), synthesized by dimethyl 2,5-furandicarboxylate, diethylene glycol (DEG) and 1,4-butanediol (BDO). Adjusting the ratio of ethyleneoxyethylene and butylene groups can endow PBD<sub>y</sub>F with excellent tensile strength (77.8 MPa), puncture resistances properties (129.7 N/mm), and barrier properties (CO<sub>2</sub> 0.0120 barrer, O<sub>2</sub> 0.0103 barrer) for PBD<sub>80</sub>F. Processing can be performed by injection moulding, and additive manufacturing, such as 3D printing. Moreover, we construct a rapid chemical-solvolysis strategy in mild conditions without producing other organic waste by the DEG/BDO to obtain recycled 2,5-furandicarboxylate, DEG, and BDO from PBD<sub>y</sub>F. Utilizing the differences of solubility and boiling point, the recycled chemicals can be separated. Repolymerized polyester (rPBD<sub>y</sub>F) still maintain high performance compared with PBD<sub>y</sub>F. In our approach, the high-performance chemical-recyclable copolyester, exhibiting greatly potential films or 3D printing applications, provides a state-of-art way for solving the trade-off problem between chemical-recycling and high performance of previous linear polyesters, further supports sustainable closed-loop chemistry.

## Experimental Procedures

### 1.1 Raw materials

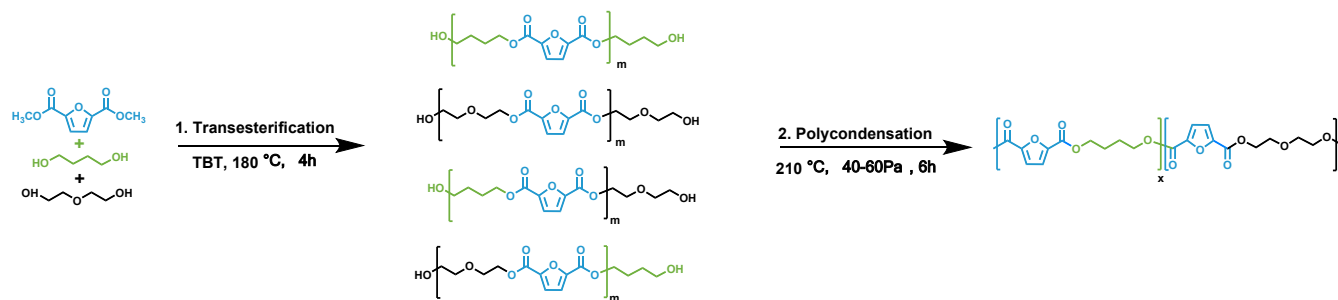
Dimethyl furan-2,5-dicarboxylate (DMFDCA), with a purity of over 99%, was purchased from ChemTarget Co., Ltd. (China). Diethylene glycol (DEG) (purity 98%) was provided by Shanghai Titan Technology Co., Ltd, China. 1,4-Butanediol (1,4-BDO) (purity  $\geq 99\%$ ) was purchased from Aladdin Reagent (Shanghai) Co., Ltd. China. Titanium(IV) n-butoxide (TBT) (purity 99%) was provided by J&K Chemical. Methyl alcohol was obtained from Tianjin Zhiyuan Chemical Reagent Co, China. Hydrochloric acid (HCl) was purchased from Kelong Chemical Factory (Chengdu, China). Sodium carbonate ( $\text{Na}_2\text{CO}_3$ ) was provided by Tianjin Bodi Technology Development Co., Ltd, China. All the other reagents were used as received without any further purification.

### 1.2 Synthesis of poly(butylene furandicarboxylate-diethylene glycol) ( $\text{PBD}_y\text{F}$ ).

In Fig. 2a, the  $\text{PBD}_y\text{F}$  was prepared by two-step procedures of transesterification and polycondensation. The  $y$  represents the molar ratio content of DEG in the diol. Five PBF,  $\text{PBD}_{20}\text{F}$ ,  $\text{PBD}_{40}\text{F}$ ,  $\text{PBD}_{60}\text{F}$ ,  $\text{PBD}_{80}\text{F}$  polyesters with different BDO/DEG molar ratios (100/0, 80/20, 60/40, 40/60 and 20/80) were synthesized in this work. The synthesis of  $\text{PBD}_{40}\text{F}$  is given as an example. 1, 4-BDO (23.8 g, 0.264 mol), DEG (18.7 g, 0.176 mol) and DMFDCA (36.8 g, 0.236 mol), TBT ( $0.08 \text{ g}$ ,  $2.4 \times 10^{-4} \text{ mol}$ , as the catalyst) were added into a 100 mL three-necked flask which was equipped with an agitator, water separator, and  $\text{N}_2$  inlet pipe. The transesterification was carried out at  $180 \text{ }^\circ\text{C}$  for 4 hours. Then the polycondensation was set at  $210 \text{ }^\circ\text{C}$  with the vacuum of 40-60 Pa for 6 hours.

#### 1.2.1 Schematic diagram of random copolymerization for $\text{PBD}_y\text{F}$

We supply a sound schematic illustration of the reaction process. In the first step (Scheme S1), the ester and diol were prepared by transesterification reaction under catalyst TBT and  $180 \text{ }^\circ\text{C}$  heating for 4 hours to form prepolymers; in the second step, the temperature was raised to  $210 \text{ }^\circ\text{C}$ , and the polycondensation reaction was performed at 40-60 Pa vacuum for 6 hours to obtain random copolyesters.



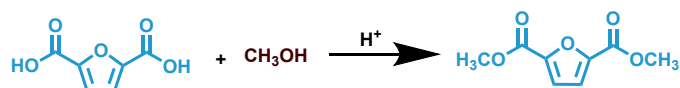
Scheme S1. Schematic diagram of random copolymerization.

### 1.3 Chemical recycling experiments

#### 1.3.1 Chemical recycling routes of $\text{PBD}_y\text{F}$

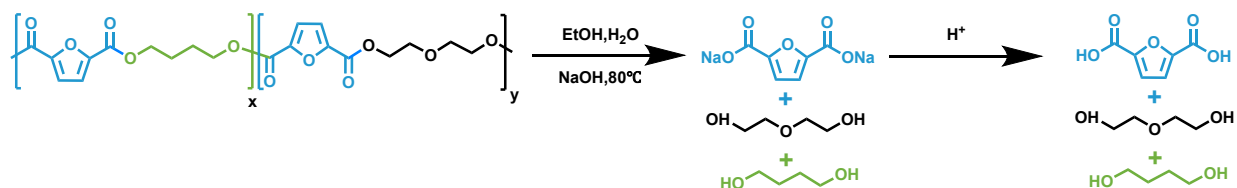
$\text{PBD}_{40}\text{F}$  was amenable to quantitative chemical recycling under mild conditions in benign solvents.  $\text{PBD}_{40}\text{F}$  (10.0 g), sodium hydroxide (NaOH) (15.5 g), water (120 mL), DEG (105 mL), and BDO (75 mL) mixture were placed into 500 mL flask with oil bath at  $80 \text{ }^\circ\text{C}$  for 1 h. Upon cooling of the reaction mixture, concentrated hydrochloric acid ( $>99\%$ ) was added to adjust the pH of the solvents to 2. Then, the sodium furandiformate can transform to recovered FDCA (rFDCA) and be separated by filtration (Scheme S3). The purify of recovered FDCA is 99.2%, and the quantitative yield is 93.7%. The residual liquid was distilled at  $120 \text{ }^\circ\text{C}$  to remove water (which can be recycled and reused), and then vacuum distillation at  $120 \text{ }^\circ\text{C}$  to obtain DEG and BDO. Thus, the BDO and DEG can also be recovered.

### 1.3.2 Synthesis of rDMFDCA by rFDCA.



Scheme S2. Schematic diagram of DMFDCA.

### 1.3.3 Schematic diagram of recycling of PBDyF copolyester.



Scheme S3. Schematic diagram of recycling of PBD<sub>y</sub>F copolyester.

### 1.3.4 Repolymerization of rPBD<sub>40</sub>F.

The recovered dimethyl 2,5-furandicarboxylate (rDMFDCA) was synthesized by rFDCA (Scheme S2) to repolymerize the recovered PBD<sub>40</sub>F (rPBD<sub>40</sub>F). rFDCA (16.7 g) and sulfuric acid (6.0 mL) were added into 150 mL methanol in a 250 mL flask with a magnetic stirrer. The mixture was stirred at 80 °C for 24 hours. After washing by deionized water and filtration, rDMFDCA is obtained. The synthesized route of rPBD<sub>y</sub>F is the same as PBD<sub>y</sub>F. The <sup>1</sup>H NMR, <sup>13</sup>C NMR, and LC data of DMFDCA are shown in the following, and their spectra are given in Fig. S9 a, b, c. <sup>1</sup>H NMR (DMSO-d<sub>6</sub>, δ, ppm): the peaks at 7.44 ppm are assigned to the H<sub>a</sub> on the furan rings. The peak at 3.87 ppm is the H<sub>b</sub> on the methyl group. <sup>13</sup>C NMR (DMSO-d<sub>6</sub>, δ, ppm): The peak at 52.9 ppm is the C<sub>a</sub> on the methyl group. The peaks at 119.5 and 146.5 ppm are assigned to the C<sub>b</sub> and C<sub>c</sub> on the furan rings. The peak at 158.3 ppm is the C<sub>d</sub> in the carbonyl group. The LC data showed the purity of DMFDCA is 98.26%.

### 1.3.5 Characterization

ATR-FTIR spectra of the polyesters were recorded on a Nicolet 6700 spectrophotometer (Thermo Fisher Scientific, USA) equipped with a germanium crystal ATR accessory in the wave-number range of 500-4000 cm<sup>-1</sup>. Before the test, the samples which needed thermal treatments were heated in a tube furnace. The intrinsic viscosities were measured by dilute solution viscometry at 30 °C. The solvent is a mixture of phenol/orthoedichlorobenzene (50:50 wt%). The chemical structures of the polyesters, FDCA and DMFDCA, were characterized by <sup>1</sup>H NMR spectroscopy and <sup>13</sup>C NMR (Bruker AC-P 400 MHz spectrometer). Deuterated trifluoroacetic acid (TFA) and Dimethyl sulfoxide-d<sub>6</sub> (DMSO-d<sub>6</sub>) were used as a solvent. The molecular weights (*M<sub>w</sub>*) and polydispersity index (PDI) of copolyesters were evaluated by gel permeation chromatography (GPC) test. The GPC test was carried out in waters1525 & Agilent PL-GPC220 with 10 mg of the sample dissolved in 10 mL of 2-chlorophenol/chloroform (1/9, v/v). With chloroform as the mobile phase, the flow rate is 1 mL min<sup>-1</sup>.

The thermal behavior of polyesters was examined by differential scanning calorimetry in a TA Instrument (DSC-Q200) under a nitrogen atmosphere. The samples of around 5 mg were placed into alumina crucibles and were scanned from 0 to 190 °C at a rate of 10 °C /min. Thermogravimetric analysis (TGA) was studied with a thermogravimetric analyzer (NETZSCH TG 209 F1 apparatus) in a nitrogen atmosphere. The samples were heated from 40 °C up to 700 °C at a 10 °C /min heating rate. The crystallinity of polyesters was characterized by wide-angle X-ray scattering (WAXS) in Panalytical X'Pert MPD Pro using copper radiation (*K*<sub>α1</sub>=1.5405980 Å), equipped with an X'Celerator-detector. Samples were scanned in the angle (2θ) range of 5-50°.

The rheological property of polyesters was characterized by a Discovery HR-2 instrument (USA) with 25 mm diameter parallel-plate geometry at 190 °C. Dynamic oscillatory shear measurements tests were performed from high to low frequency over a 0.01-100 Hz range, at strains of 1%, with a gap size of 1 mm.

---

The positron annihilation lifetime spectrometer (model PLS-System) was obtained by measurement of positron annihilation lifetime spectroscopy (PALS). The PBF and PBD<sub>y</sub>F membranes are amorphous states confirmed by the WAXS (Fig. S9 d). Two small discs of 25 mm×25 mm×1 mm were placed between the <sup>22</sup>Na positron source, and the time resolution of the positron source was 0.23 ns. The time delay between the emission of one of the birth gamma (1.28 MeV) and 0.511 MeV annihilation photons can determine the positron lifetime.

The tensile strength and elongation at break of PBD<sub>y</sub>F membrane were measured on an Instron Universal Testing Machine (model 5567) at a 15 mm/min crosshead speed at room temperature. Repeated testing of five specimens for each sample and reported the average result. The puncture resistance of the PBD<sub>y</sub>F membrane was characterized by MTS (USA) CMT2205 universal testing machine according to the standard GB/T 37841-2019. The probe moves at a 50 mm/min speed, and the puncture strength was given with a unit of N/mm.

Barrier properties to O<sub>2</sub> and CO<sub>2</sub> were tested through a manometric method using a permeance testing device (Labthink VAC-V2). All melt-pressed membranes of polyesters were cut into circular discs with a thickness of 0.5 mm and a diameter of 50 mm. Each measurement was continuously monitored until a stable oxygen permeability rate was reached.

The transparency and haze of the PBD<sub>y</sub>F membrane samples were evaluated by a transparency-haze meter (PE Company, model Lambda750).

The purity of rFDCA and rDMFDCA were characterized by liquid chromatography (LC) and liquid chromatograph-mass spectroscopy (LC-MS) with Finnigan TSQ Quantum. The recycled liquid was tested by Gas Chromatograph (GC) with Agilent 7890B using methanol as solvent, and the test condition was to keep the temperature at 60 °C for 3 minutes and increase to 240 °C at 20 °C per minute.

## Results and Discussion

### Structural characterization

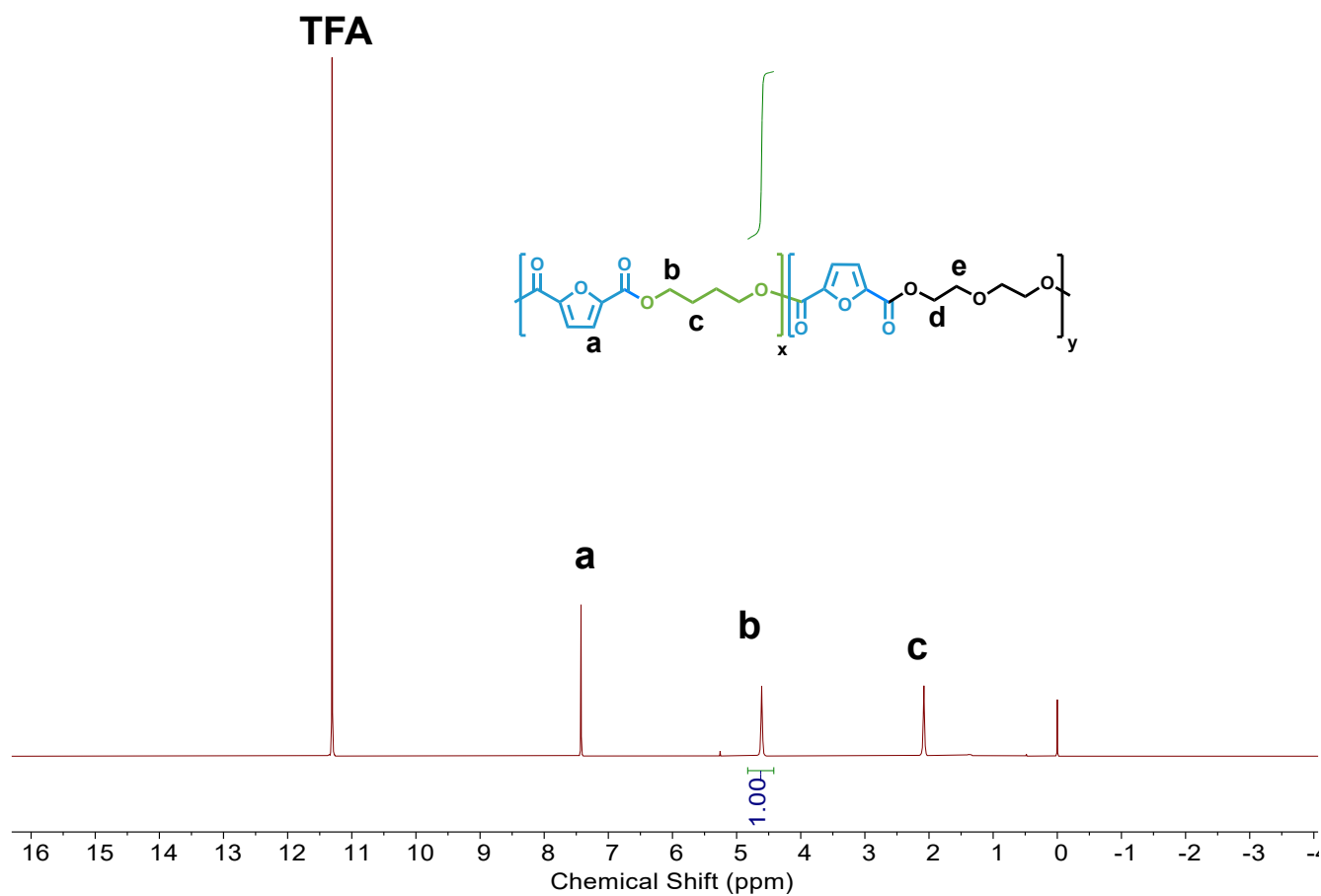


Figure S1.  $^1\text{H}$  NMR spectrum of PBF.

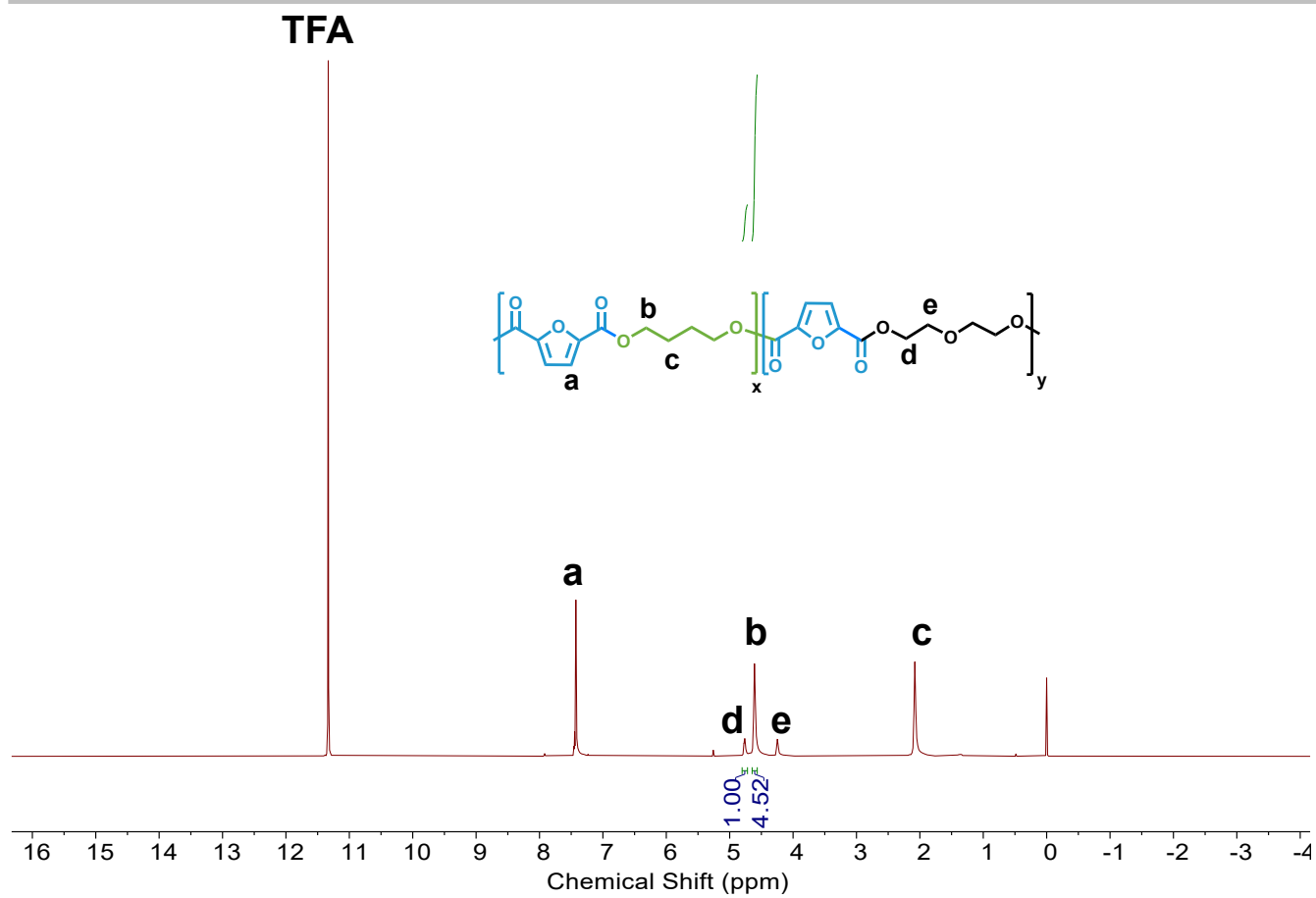


Figure S2. <sup>1</sup>H NMR spectrum of PBD<sub>20</sub>F copolyesters.

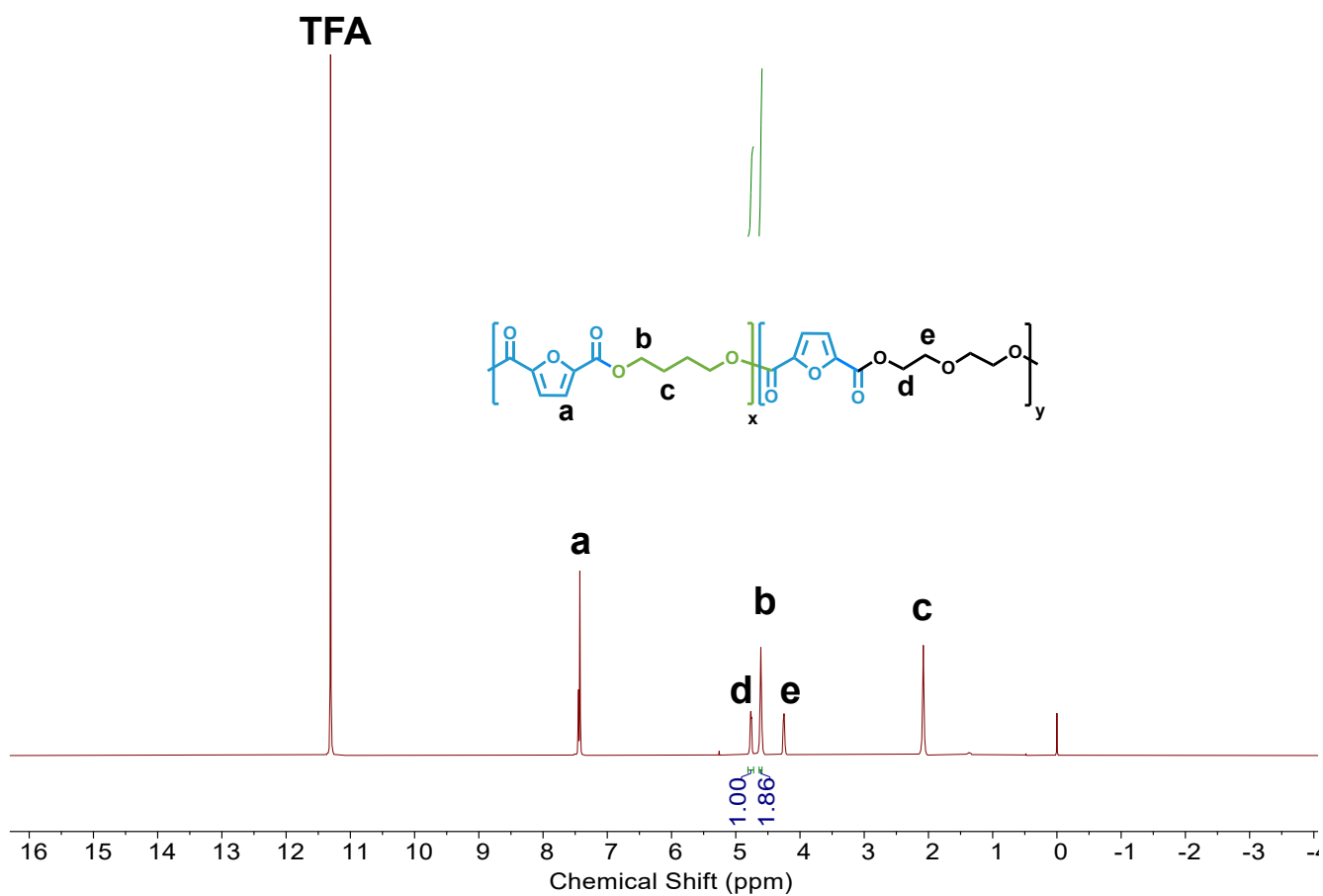


Figure S3.  $^1\text{H}$  NMR spectrum of PBD<sub>40</sub>F copolyesters.

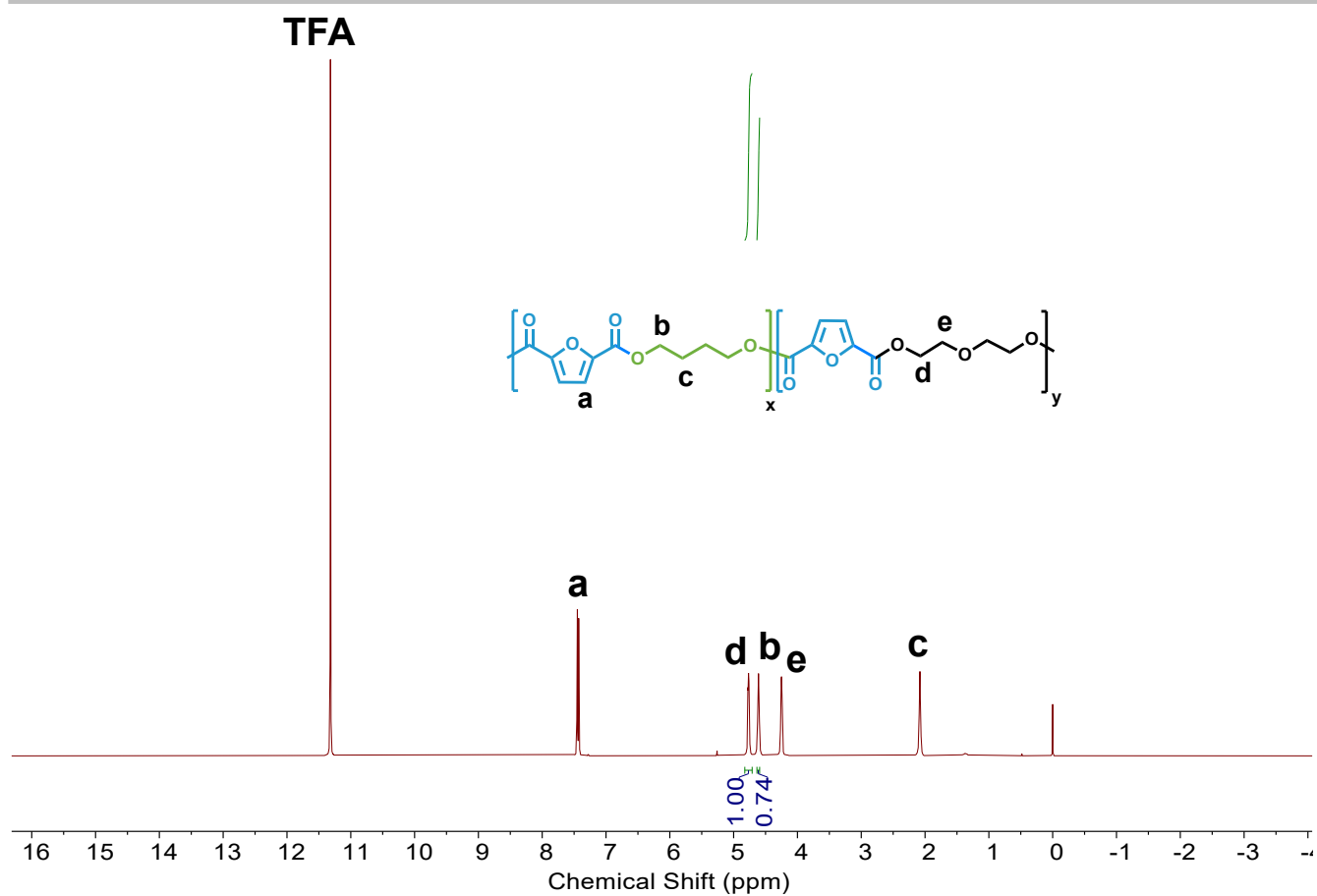


Figure S4.  $^1\text{H}$  NMR spectrum of PBD<sub>60</sub>F copolyesters.

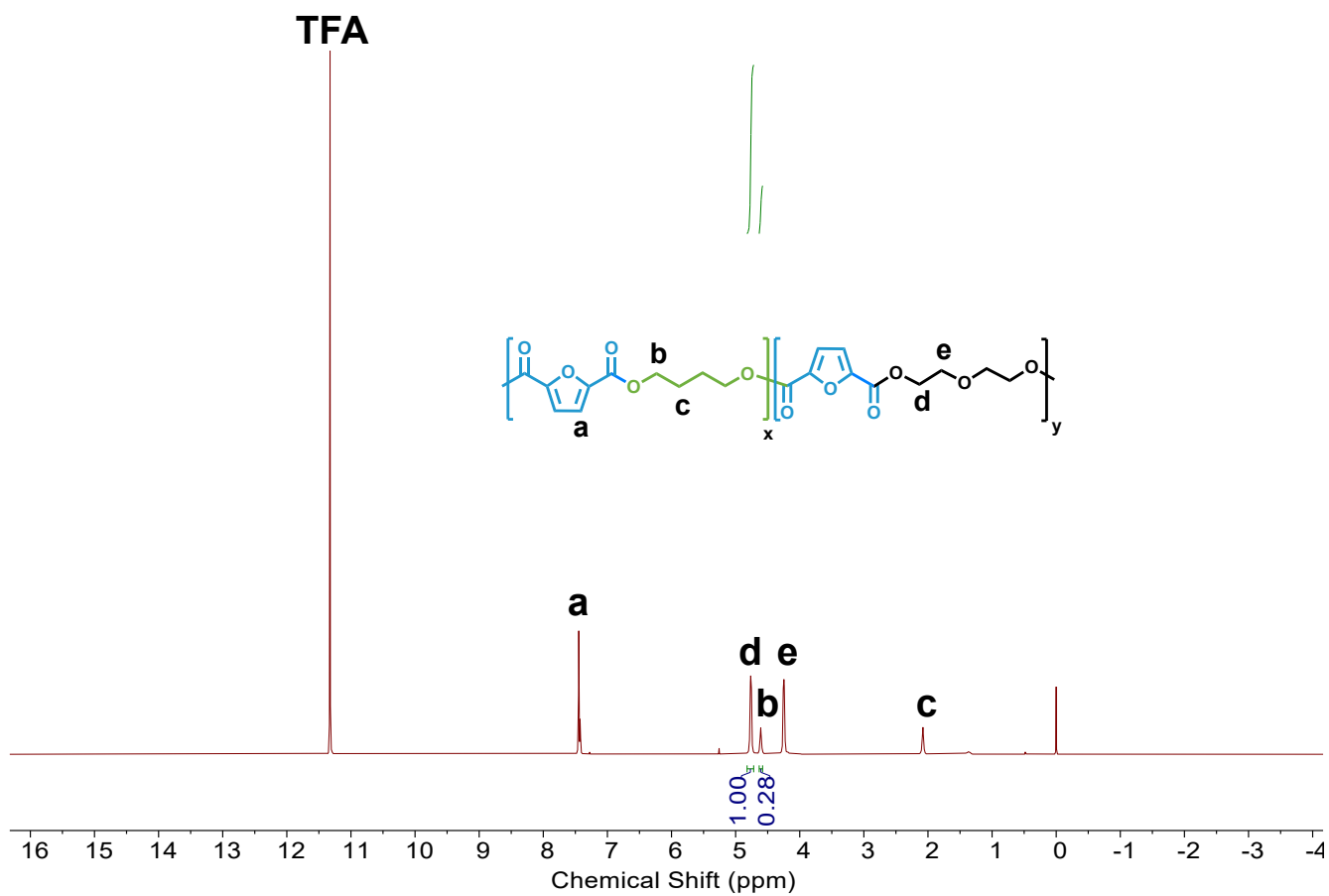


Figure S5.  $^1\text{H}$  NMR spectrum of PBD<sub>80</sub>F copolyesters.

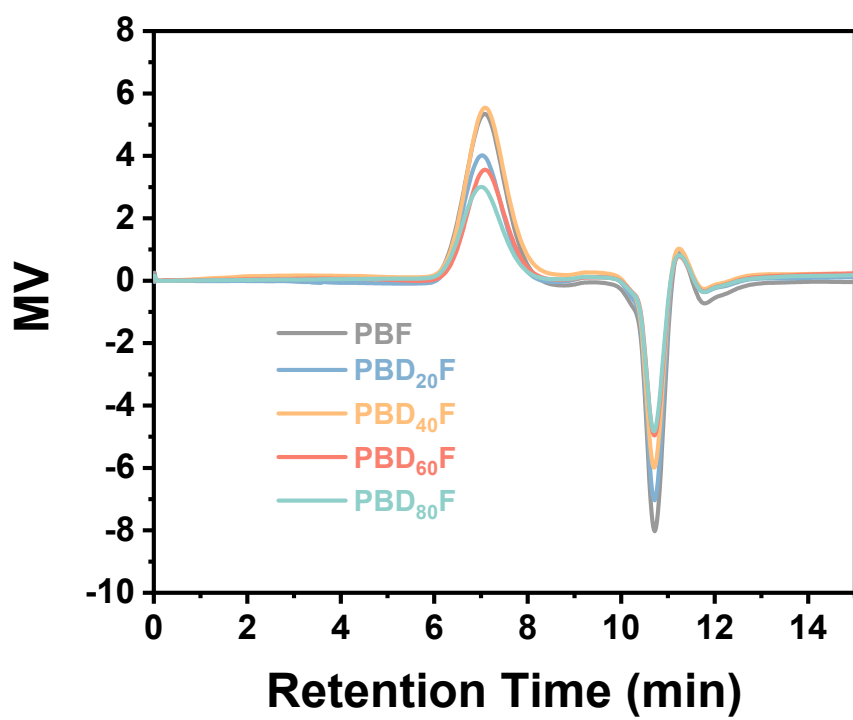


Figure S6. GPC chromatogram of PBF and PBD<sub>x</sub>F copolyesters.

## Thermal properties

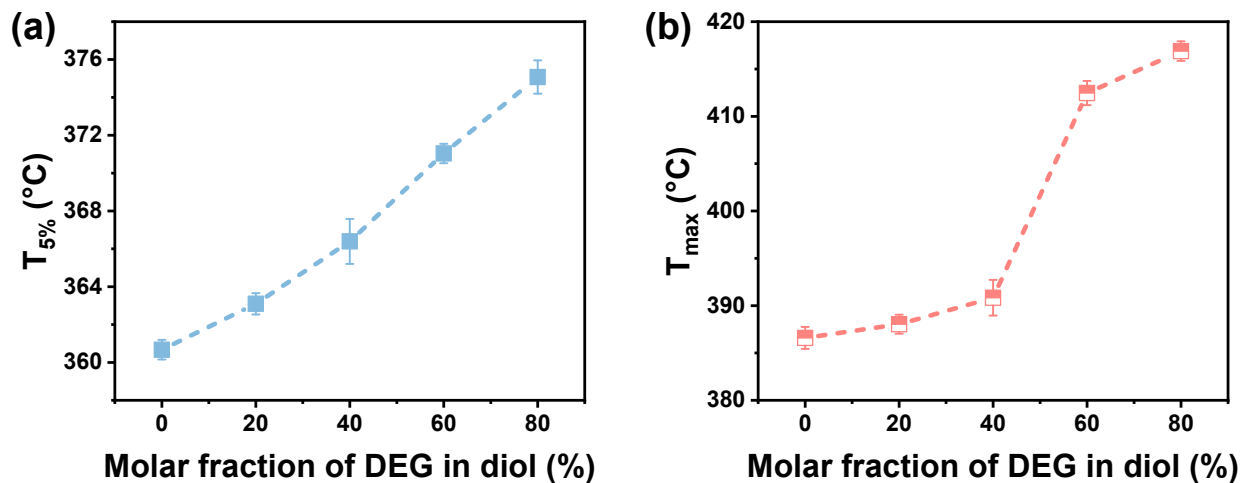


Figure S7. (a)  $T_{5\%}$  with error bars for PBF and PBD<sub>y</sub>F copolyesters, (b)  $T_{max}$  with error bars for PBF and PBD<sub>y</sub>F copolyesters.

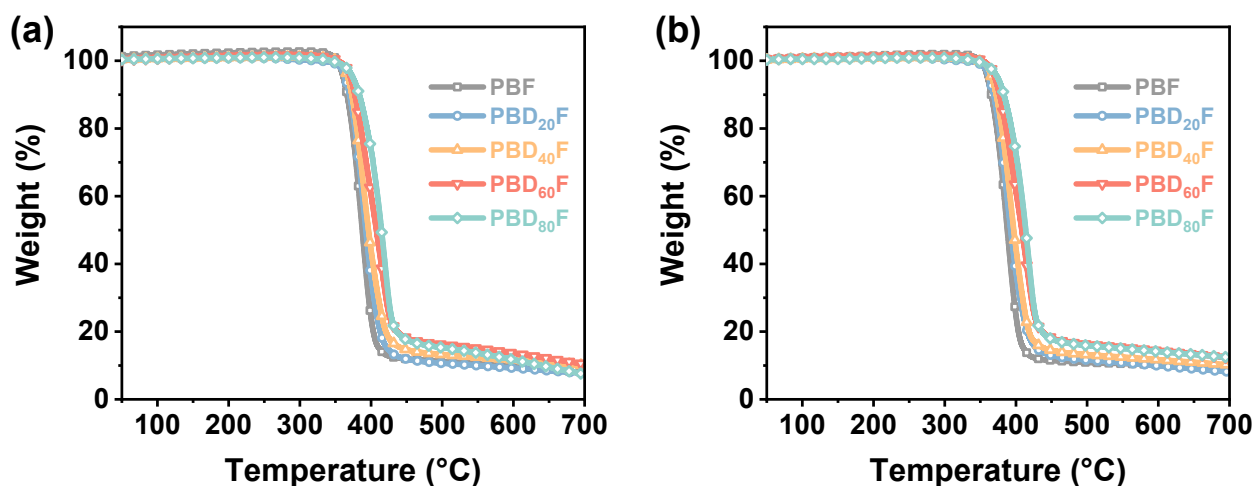


Figure S8. TGA curves of PBF and PBD<sub>y</sub>F copolyesters.

---

### Positron annihilation lifetime spectrum (PALS)

Usually, there are two types of positrons in polymer materials, namely the pair state (*p*-Ps, singlet spin state) and the ortho state (*o*-Ps, triplet spin state). Among them, *p*-Ps undergoes self-annihilation decay by emitting two kinds of gamma rays, with a lifetime of 125 ps. The self-annihilation lifetime of the three gamma rays emitted by *o*-Ps is 142 ns. When Ps collides with a molecule, *o*-Ps will pick up an electron from the surrounding molecules and annihilate it by emitting two beams of gamma rays, this phenomenon is called "pick-off" annihilation, which is highly sensitive to the size of the free volume.<sup>1</sup> When annihilation occurs, the test will generate data for three exponential decay components (Lifetime 1  $\tau_1$ , Lifetime 2  $\tau_2$ , and Lifetime 3  $\tau_3$ ), where  $\tau_1$  is due to the *p*-Ps lifetime and free annihilation lifetime of positrons. The component  $\tau_2$  is attributed to the annihilation of positrons in the amorphous region.  $\tau_3$  can be used to calculate the free volume of amorphous materials, which is attributed to the "pick-off" annihilation of *o*-Ps at the pores in the amorphous phase. Table S1 is the data obtained from a detailed analysis of the life spectrum. The radius  $R$  of the free volume can be calculated by Eq S1.<sup>2</sup>

$$\tau_3 = \frac{1}{2} \left[ 1 - \frac{R}{R + \Delta R} + \frac{1}{2\pi} \sin \left( \frac{2\pi R}{R + \Delta R} \right) \right] \quad (1)$$

In Eq S1,  $\Delta R$  is the thickness of the electron layer, and it is known from the literature that its value is 0.166nm.<sup>3</sup> As shown in Table S1, the *o*-Ps intensity ( $I_3$ ) of the PBD<sub>y</sub>F copolyesters exhibited a decreasing order with increase of DEG contents, which means that the number of free volume cavities decreases accordingly. The free volume ( $F_V$ ) of the polymer can be expressed by Eq S2, which value is related to the size and number of cavities.

$$F_V = C \frac{4\pi}{3} R^3 I_3 \quad (2)$$

In Eq S2,  $C$  is the scaling factor for spherical hole, which the value is 1.5.<sup>4</sup>

## Gas barrier properties

In Table S1, the CO<sub>2</sub> and O<sub>2</sub> permeability of the as-prepared PBD<sub>80</sub>F are compared with those of previously reported polyesters. The Barrier Improvement Factor (BIFp), represents the permeability coefficient of CO<sub>2</sub> and O<sub>2</sub> in PBAT divided by the CO<sub>2</sub> and O<sub>2</sub> permeability in other materials. Obviously, all PBD<sub>y</sub>F samples have higher CO<sub>2</sub> and O<sub>2</sub> barrier property than PBAT, PLA and PET, which the BIFp was determined to be 153.2~491.7 for CO<sub>2</sub> and 60.3~73.8 for O<sub>2</sub>, respectively.

**Table S1.** Gas Permeability Coefficients for PBF and PBD<sub>y</sub>F Copolyesters

Sample <sup>[a]</sup>	CO <sub>2</sub> (barrer) <sup>[b]</sup>	BIFp	O <sub>2</sub> (barrer) <sup>[c]</sup>	BIFp
PBAT <sup>5</sup>	5.9	1.0	0.76	1.0
PLA <sup>5</sup>	1.0	5.9	0.25	3.0
PET <sup>6</sup>	0.099	59.6	0.060	12.7
PNF <sup>7</sup>	0.0310	190.3	0.0150	50.7
PBCF-20 <sup>8</sup>	0.0260	226.9	0.0240	31.7
PBCF-40 <sup>9</sup>	0.1600	36.875	0.0150	50.7
PBFGA <sub>10</sub> <sup>10</sup>	0.0500	118.0	0.0210	36.2
Pl <sub>80</sub> CBF <sub>10</sub> S <sub>10</sub> <sup>11</sup>	0.1900	31.1	0.2000	3.8
PBO <sub>61</sub> F <sub>39</sub> <sup>12</sup>	0.0470	125.5	0.0720	10.6
PNDF <sub>90</sub> <sup>13</sup>	0.0350	168.6	0.0330	23.0
PNSF <sub>60</sub> <sup>5</sup>	0.0300	196.7	0.0240	31.7
PBFLA <sub>10</sub> <sup>14</sup>	0.0570	103.5	0.0150	50.7
PBF	0.0385	153.2	0.0126	60.3
PBD <sub>20</sub> F	0.0329	179.3	0.0121	62.8
PBD <sub>40</sub> F	0.0255	231.4	0.0117	65.0
PBD <sub>60</sub> F	0.0209	282.3	0.0111	68.5
PBD <sub>80</sub> F	0.0120	491.7	0.0103	73.8

[a] The test was performed at 0.1 MPa. [b] CO<sub>2</sub> permeability coefficient, at 23 °C, 50% relative humidity 1 barrer = 10<sup>-10</sup> cm<sup>3</sup>cm/cm<sup>2</sup>•s•cm Hg. [c] O<sub>2</sub> permeability coefficient, at 23 °C, 50% relative humidity. Data from refs [5-14].

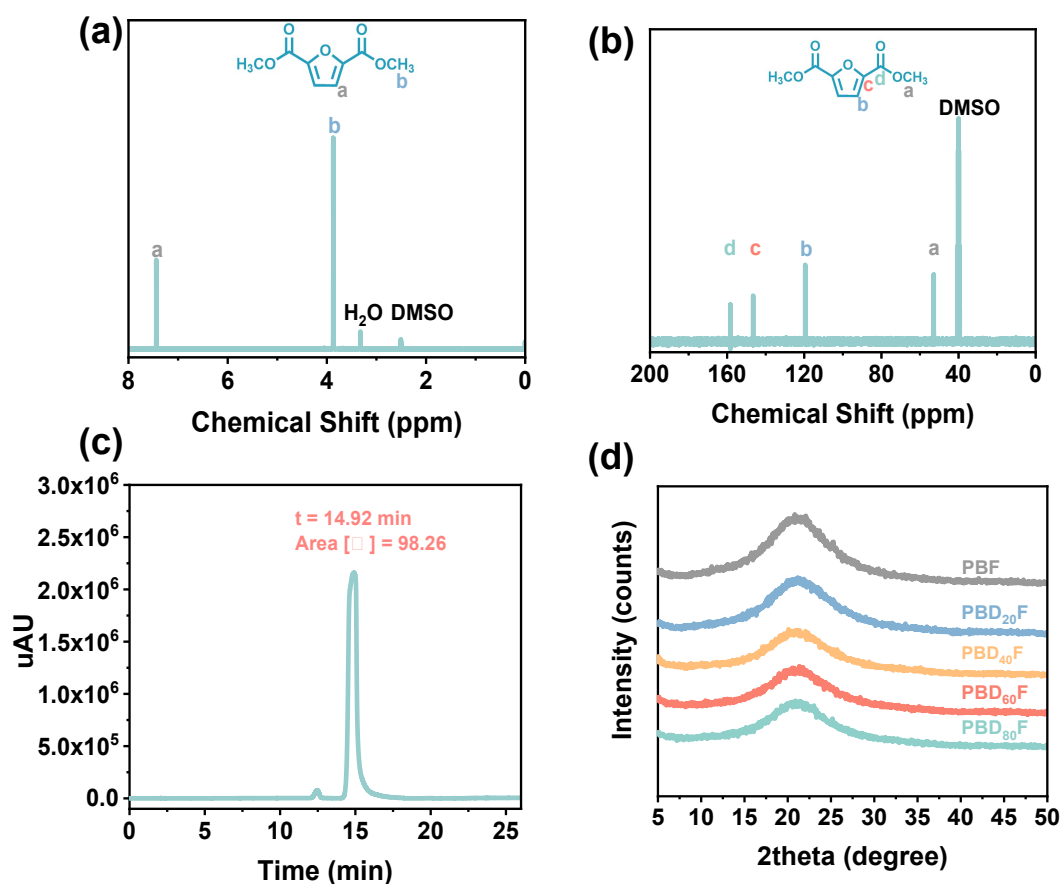


Figure S9. (a)  $^1\text{H}$  NMR spectra, (b)  $^{13}\text{C}$  NMR spectra and (c) LC trace of DMFDCA obtained from recycling experiment. (d) XRD patterns of unannealed PBF and PBD $_n$ F copolyesters.

### Mechanical Properties of rPBD $_{40}$ F polyester

After methyl esterification of the recycled FDCA, rPBD $_{40}$ F was obtained through transesterification and polycondensation. Typical tensile stress-strain curves of rPBD $_{40}$ F polyester are shown in Fig. S2. The tensile strength, elongation at break, and elastic modulus are listed in Table S2. The data shows that rPBD $_{40}$ F polyester still has excellent tensile strength and elongation at break, which indicating that the monomer obtained by the recycle experiment in this article can be recycled many times, and the recycle method in this article is feasible and efficient.

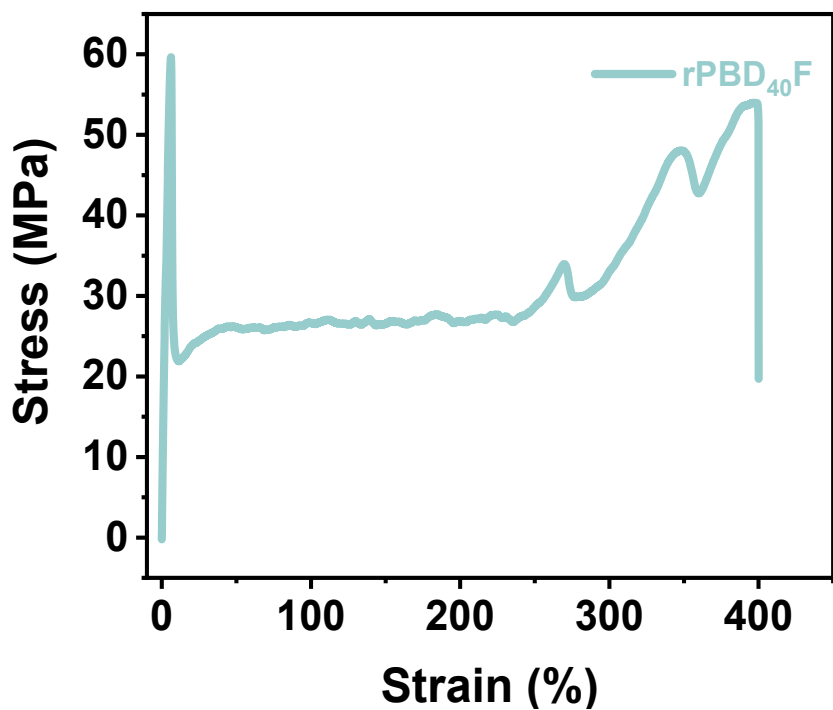


Figure S10. Stress-strain curves of rPBD<sub>40</sub>F copolyester.

Table S2. Mechanical Properties of rPBD<sub>40</sub>F Copolyester

Sample	Tensile strength (MPa)	Elongation break (%)	Elastic modulus (MPa)
rPBD <sub>40</sub> F	58.8±0.6	399.9±11.2	1433.8±34.2
PBD <sub>40</sub> F	59.9±2.0	288.7±19.2	2427.3±184.2

---

## Notes and references

- 1 C. Qian, R. Bei, T. Zhu, W. Zheng, S. Liu, Z. Chi, M. P. Aldred, X. Chen, Y. Zhang and J. Xu, *Macromolecules*, 2019, **52**, 4601-4609.
- 2 G. Dlubek, K. Saarinen and H. Fretwell, *Journal of Polymer Science Part B: Polymer Physics*, 1998, **36**, 1513-1528.
- 3 V. Shantarovich, I. Kevdina, Y. P. Yampolskii and A. Y. Alentiev, *Macromolecules*, 2000, **33**, 7453-7466.
- 4 G. G. Hougham and Y. C. Jean, *Macromolecular Chemistry and Physics*, 2014, **215**, 103-110.
- 5 H. Hu, R. Zhang, Y. Jiang, L. Shi, J. Wang, W. B. Ying and J. Zhu, *ACS Sustainable Chemistry & Engineering*, 2019, **7**, 4255-4265.
- 6 T. P. Kainulainen, J. A. Sirviö, J. Sethi, T. I. Hukka and J. P. Heiskanen, *Macromolecules*, 2018, **51**, 1822-1829.
- 7 J. Wang, L. Sun, Z. Shen, J. Zhu, X. Song and X. Liu, *ACS Sustainable Chemistry & Engineering*, 2019, **7**, 3282-3291.
- 8 A. Shen, G. Wang, J. Wang, X. Zhang, X. Fei, L. Fan, J. Zhu and X. Liu, *European Polymer Journal*, 2021, **147**.
- 9 H. Hu, R. Zhang, J. Wang, W. B. Ying and J. Zhu, *ACS Sustainable Chemistry & Engineering*, 2018, **6**, 7488-7498.
- 10 H. Hu, R. Zhang, J. Wang, W. B. Ying, L. Shi, C. Yao, Z. Kong, K. Wang and J. Zhu, *Green Chemistry*, 2019, **21**, 3013-3022.
- 11 Q. Ouyang, J. Liu, C. Li, L. Zheng, Y. Xiao, S. Wu and B. Zhang, *Polymer Chemistry*, 2019, **10**, 5594-5601.
- 12 H. Zhang, M. Jiang, Y. Wu, L. Li, Z. Wang, R. Wang and G. Zhou, *ACS Sustainable Chemistry & Engineering*, 2021, **9**, 6799-6809.
- 13 H. Hu, J. Li, Y. Tian, S. Luo, J. Wang, W. B. Ying, F. Li, C. Chen, Y.-L. Zhao, R. Zhang and J. Zhu, *ACS Sustainable Chemistry & Engineering*, 2021, **9**, 13021-13032.
- 14 H. Hu, R. Zhang, L. Shi, W. B. Ying, J. Wang and J. Zhu, *Industrial & Engineering Chemistry Research*, 2018, **57**, 11020-11030.